Polarization-insensitive low-crosstalk 8 × 8 silicon photonics switch with 9 × 13.5 cm^2 control board

R. Konoike, H. Matsuura, K. Suzuki, H. Kawashima, K. Ikeda

National Institute of Advanced Industrial Science and Technology (AIST), 1-1-1 Umezono, Ibaraki, Japan, r.konoike@aist.go.jp

Abstract *An on-chip polarization-diversity 8 × 8 silicon photonics switch with PDL < 0.4 dB, DGD < 1.8 ps and crosstalk < -30 dB over 70-nm bandwidth is demonstrated. The USB-controlled switch module has a compact size of 9 × 13.5 cm*^{2}*.*

Introduction

Optical switches with fast switching are of great importance in next generation optical networks in telecom and datacom [1-2]. Silicon photonics switches are one of the key devices as they offer a short switching time of μsec order, mass productivity, reliability and compactness [3-5]. However, they also have issues of polarization dependency, relatively large crosstalk, and lack of compact packaging including the control board. For wide usability of the optical switch, these issues need to be solved. As compared to waveguide-based MEMS switches [3], Thermo-Optic Mach-Zehnder Interferometer (TO-MZI)-based switches [4] can be driven with relatively low voltages which leads to compact and low-cost driver circuits [5]. We have recently developed low crosstalk silicon photonics switches based on a double-MZI configuration [6] with fibre-based polarization-diversity circuits [4]. However, it requires two sets of switch and control board and a number of costly PM-fibre components, increasing the complexity of the packaging and control. In this paper, we develop both the chip and the control board that allow polarization-insensitive, low-crosstalk 8 × 8 optical switching with an ultra-compact module size of 9 × 13.5 cm^2. We demonstrate a novel on-chip polarization diversity switch configuration combined with the double-MZI architecture which allows a low PDL of less than 0.4 dB, a low DGD of less than 1.8 ps, and a low crosstalk of less than -30 dB over a wavelength range wider than C-band. All of the 512 heaters on the chip were controlled through two FPGAs and a CPU on a control board with an USB interface to connect to a computer. Our demonstration leads to practical usefulness of silicon photonics switches.

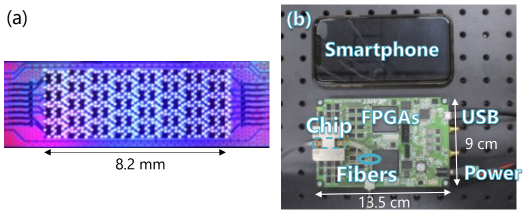

Fig. 2: (a) Micrograph of a chip. **(b)** Developed module.

Dsign, fabrication, and packaging

Figure 1(a) shows a schematic illustration of the 8 × 8 switch chip. The switch is based on the Path-Independent insertion Loss (PILOSS) topology [7]. For the polarization diversity configuration, we have two identical switch circuits for the two orthogonal polarization components (TE and TM) on a chip. We used the Polarization Splitter-Rotator (PSR) which splits the TE/TM components and rotates the TM light into TE light as shown in Fig. 1(a). Here, we call the rotated light as (originally-)TM light. The blue and red lines show switch circuits for the TE and TM light, respectively. The detailed structure of each 2 × 2 switch unit is shown in Fig. 1(b). Here, we have two sets of double-MZI switch unit for low-crosstalk characteristic. The reason of low-crosstalk in this structure can be understood as

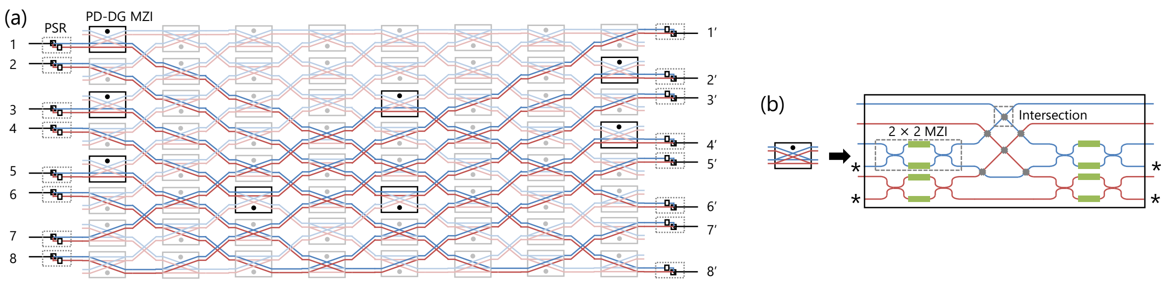

Fig. 1: (a) Schematic illustration of the 8 × 8 switch chip with example connections. The ‘cross’ or ‘off’ switches are depicted by gray blocks, and ‘bar’ or ‘on’ switches are depicted by black blocks. **(b)** Detailed structure of the 2 × 2 switch unit. Ports with asterisks (*) are idle ports.

follows. First, the leakage of MZI is large when it is in the cross state. In the double-MZI configuration, the leaked light is always guided to the idle ports. The path lengths of the blue/red circuits are designed to be the same in order to suppress the DGD. The switch was fabricated in AIST's 300-mm CMOS pilot line equipped with ArF immersion lithography. A micrograph of the fabricated chip is shown in Fig. 2(a). The chip was then flip-chip bonded to a ceramic interposer with 576-pin Land Grid Array (LGA). It is then inserted into a LGA socket on the developed control circuit board whch is shown in Fig. 2(b). The control board contains two FPGAs (Cyclone® V), a CPU (R8C) for the communication with a computer, buffer ICs for the PWM control of the heaters, and power supply circuits. As shown in this figure, the module size is 9 × 13.5 cm^2 which is as small as a smartphone as shown in Fig. 2(b).

Measurement of PSR

We first measured the characteristics of the PSR. The detailed structure of the PSR is shown in Fig. 3(a). The PSR is based on the TM-TE mode coupling as shown in [8]. The originally-TE light passes through the lower waveguide of Fig. 3(a). The originally-TM light (red arrow) is converted into TE1 mode in the thick waveguide (orange arrow) through the tapered region. For this TM-TE conversion, half-etched SOI rib structure was used. The TE1 mode is then coupled to TE0 mode of the narrow waveguide through the directional coupling region as shown in Fig. 3(a). A test structure shown in Fig. 3(b) was prepared to check the PDL of the fabricated PSR. The results, together with the insertion loss of the two PSRs, are plotted in Fig. 3(c) in blue (TE), red (TM) lines and black markers. From this figure, we can see that the PDL was very small (less than 1 dB, which is limited by Fabry-Pérot fringes) with the insertion loss of ~2.0 dB for the set of two PSRs at 1557 nm. The reason of large loss at the longer wavelength is due to the wavelength dependency of the directional coupler.

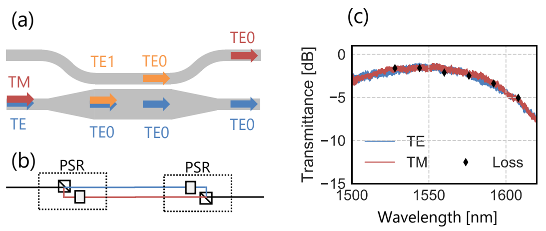

Fig. 3: (a) Structure of the PSR. **(b)** Structure of the test device. **(c)** Measured TE/TM spectra and loss of the PSRs.

All-path loss measurement

As the first step of the device characterization, the initial phase errors of all the MZIs on the chip was trimmed out. We developed PC control software for the trimming/control of the switch. We trimmed all the MZIs manually. We then performed all-path fibre-to-fibre (FtF) insertion loss (IL) measurement. The results are shown in Fig. 4. The 8 separate panels correspond to input ports 1 to 8. The *x*-axis of the graph corresponds to the measured output port and the eight colors (shown in the legend) correspond to the target output ports. The circles show the results when input TE-polarized light and the squares show the results when input TM-polarized light. The points around -10 dB show switch ILs and the points below -50 dB show leakages to untargeted ports. We note that initially the TE and TM ILs were slightly (<1 dB) different due to fabrication error. In order to minimize the PDL, we adjusted the cross state of the second MZI (right-sided MZIs in Fig. 1(b)) so that the light partially dissipated into the unused ports, and TE and TM ILs match each other. As a result, the minimum / maximum / average FtF IL was 11.0 / 12.8 / 11.9 dB, respectively, with path-dependent PDL of less than 0.05 dB at 1557 nm. The breakdown of the minimum loss is as follows. Fiber-to-chip coupling loss: 2.4 dB / facet, on-chip guiding loss: 0.6 dB, PSR loss: 2.0 dB, 2 × 2 switch unit loss: 0.45 dB/unit. The fiber-to-chip coupling loss was measured using a pass-through waveguide fabricated on the same chip.

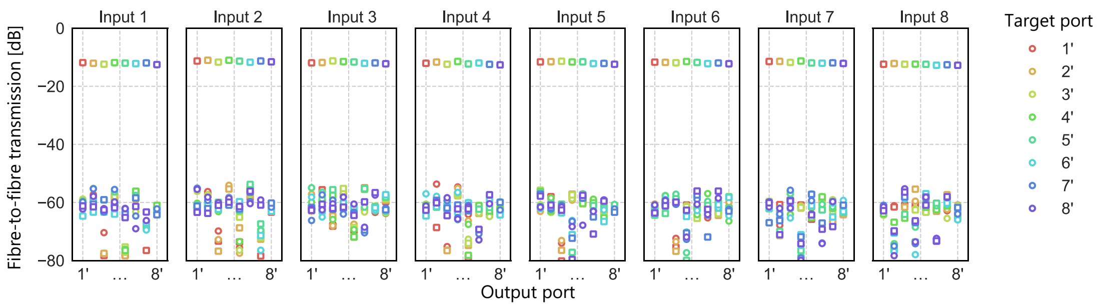

Fig. 4: Measured all-path fibre-to-fibre transmission loss.

PDL/DGD measurement

Next, we measured the PDL/DGD spectrum of the path 7 → 6'. For the PDL measurement, we input ASE light which is polarized into TE/TM by using an inline polarizer and a fiber polarization controller. The output spectra were measured using optical spectrum analyzer and the PDL spectrum was calculated. Fig. 5(a) shows the measured PDL spectrum. As shown in this figure, the PDL was less than 0.4 dB from 1520 nm to 1600 nm. We consider that the PDL is caused by reflections on the chip. We then measured the DGD spectrum of the same path with using a component analyzer (Keysight N7788B). As shown in the results of Fig. 5(b), the DGD was less than 1.8 ps.

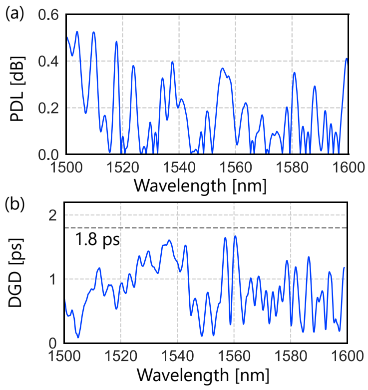

Fig. 5: (a) Measured PDL and **(b)** DGD spectra.

Crosstalk measurement

We finally measured the crosstalk spectrum of one of the largest crosstalk paths. The path setting shown in Fig. 1(a) is one of the largest crosstalk paths of the switch where the main path is 7 → 6'. We input tunable CW light into the 8 paths of Fig. 1(a) and measured the transmittance of the main path and the leakages from other paths to the main path. The results are shown in Fig. 6(a). As shown in this figure, the leakages were suppressed by more than 40 dB thanks to the double-MZI configuration. The crosstalk value is calculated as a difference between the main path transmittance and the sum of the leakages. The result is shown in Fig. 6(b). The broad bandwidth of ~90 nm was obtained with the worst-case crosstalk of less than -30 dB.

Conclusions

In this paper, we have demonstrated the on-chip polarization diversity low crosstalk 8 × 8 silicon photonics switch with the ultra-compact module size of 9 × 13.5 cm^2. A novel design of on-chip polarization diversity switch circuit allowed low PDL of less than 0.4 dB and low DGD of less than 1.8 ps with broad bandwidth. The worst-case crosstalk was less than -30 dB from 1500 nm to 1590 nm. The insertion loss could be further reduced by >2 dB with optimization of the fibre-to-chip coupling region [9].

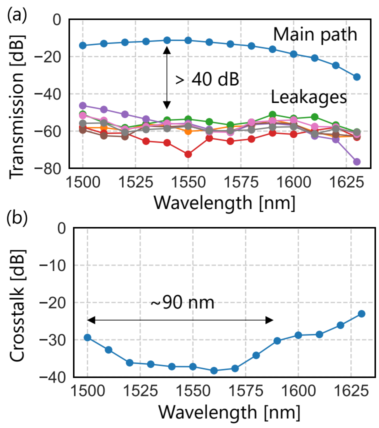

Fig. 6: (a) Measured transmission loss of the main path and the leakages to the main path. **(b)** Worst-case crosstalk spectrum calculated from (a).

Acknowledgements

The device was fabricated in SCR of AIST.

References

[1] K. Ishii, J. Kurumida, S. Namiki, et al., "Energy consumption and traffic scaling of dynamic optical path networks," Proc. SPIE, San Diego, US, December 2013, p. 86460A

[2] K. Ueda, et al., "Novel Intra- and Inter-Datacenter Converged Network Exploiting Space- and Wavelength-Dimensional Switches," Proc. OFC, Los Angeles, US, March 2017, p. M3K.2.

[3] T. J. Seok, et al., "Highly Scalable Digital Silicon Photonic MEMS Switches," J. Lightwave Technol. 34, pp.365-371 (2016).

[4] K. Suzuki, K. Tanizawa, S. Suda, et al., "Broadband silicon photonics 8×8 switch based on double-Mach-Zehnder element switches," Opt. Express, 2017, 25, (7), pp. 7538-7546

[5] H. Matsuura, S. Suda, et al., "Accelerating Switching Speed of Thermo-optic MZI Silicon-Photonic Switches with "Turbo Pulse" in PWM Control," Proc. OFC, Los Angeles, US, March 2017, p. W4E.3

[6] T. Goh, et al., "High-Extinction Ratio and Low-Loss Silica-Based 8 × 8 Strictly Nonblocking Thermooptic Matrix Switch," J. Lightwave Technol. 17, pp. 1192-1199 (1999).

[7] T. Nishi, et al., "A polarization-controlled free-space photonic switch based on a PI-LOSS switch," IEEE Photonics Technology Letters 5, pp. 1104-1106 (1993).

[8] D. Dai and J. E. Bowers, "Novel concept for ultracompact polarization splitter-rotator based on silicon nanowires," Opt. Express 19, pp. 10940-10949 (2011).

[9] K. Suzuki, et al., "Low-Inerstion-Loss and Power-Efficient 32 × 32 Silicon Photonics Switch With Extremely High-Δ Silica PLC Connector," J. Lightwave Technol. 37, pp. 116-122 (2019).